Journal of Power Sources 327 (2016) 265–272

Contents lists available at ScienceDirect

Journal of Power Sources

journal homepage: www.elsevier.com/locate/jpowsour

Preparation and characterization of mono-sheet bipolar membranes by pre-irradiation grafting method for fuel cell applications

Yingjie Guan, Jun Fang*, Tao Fu, Huili Zhou, Xin Wang, Zixiang Deng, Jinbao Zhao

Department of Chemical & Biochemical Engineering, College of Chemistry and Chemical Engineering, Xiamen University, Xiamen 361005, PR China

HIGHLIGHTS

- Novel mono-sheet bipolar membrane was prepared by pre-irradiation grafting method.
- The membranes showed good stability, ionic conductivity and ion exchange capacity.
- The thickness of anion/cation exchange layer of the membrane can be easily controlled.
- The properties of the membranes can be tuned by varying the degree of grafting.
- The membranes were successfully used in the fuel cells without humidification.

ARTICLE INFO

Article history:
Received 18 May 2016
Received in revised form
13 July 2016
Accepted 16 July 2016
Available online 25 July 2016

Keywords:
Mono-sheet bipolar membrane
Bipolar membrane fuel cell
Radiation grafting
ETFE

ABSTRACT

A new method for the preparation of the mono-sheet bipolar membrane applied to fuel cells was developed based on the pre-irradiation grafting technology. A series of bipolar membranes were successfully prepared by simultaneously grafting of styrene onto one side of the poly(ethylene-*co*-tetrafluoroethylene) base film and 1-vinylimidazole onto the opposite side, followed by the sulfonation and alkylation, respectively. The chemical structures and microstructures of the prepared membranes were investigated by ATR-FTIR and SEM-EDS. The TGA measurements demonstrated the prepared bipolar membranes have reasonable thermal stability. The ion exchange capacity, water uptake and ionic conductivity of the membranes were also characterized. The H_2/O_2 single fuel cells using these membranes were evaluated and revealed a maximum power density of 107 mW cm^{-2} at 35 °C with unhumidified hydrogen and oxygen. The preliminary performances suggested the great prospect of these membranes in application of bipolar membrane fuel cells.

1. Introduction

Polymer electrolyte membrane fuel cells, including conventional proton exchange membrane fuel cells (PEMFCs) and anion exchange membrane fuel cells (AEMFCs), have received considerable interest in recent decades. Although PEMFCs were identified as the prospective power sources for power generating stations, vehicular transportations, and portable power supply, there are still some obstacles to their commercialization such as sluggish oxygen reduction kinetics, complex water management and the high cost of the critical materials. AEMFCs may offer plenty of potential advantages, such as more facile electrokinetics, wider selection of catalyst, and lower fuel (e.g. alcohols) crossover. The most encouraging aspect of AEMFCs is the cost of the fuel cell may be greatly reduced, because the non-noble metals, such as silver and nickel are allowed to be used as catalysts in the alkaline working condition. However, compared with PEMFCs, the poor ionic conductivity of the anion exchange membranes (AEMs) is a serious problem because it may lower the performance of the AEMFCs.

In an effort to use the proton exchange membrane which has high conductivity and still exploit the potential electrochemical advantages of the alkaline operating condition, recently, Kohl and his coworkers [1–6] described the use of the bipolar polymer electrolyte interfaces for H_2/O_2 and direct methanol fuel cells. Although the power densities reported were relatively low, the bipolar membrane fuel cells are theoretically promising because they not only combine the advantages of PEMFCs and AEMFCs, but also have the function of self-humidification. The membrane electrode assembly (MEA) is the core component of the self-

---

* Corresponding author.
E-mail address: jfang@xmu.edu.cn (J. Fang).

http://dx.doi.org/10.1016/j.jpowsour.2016.07.060
0378-7753/

humidifying bipolar membrane fuel cell, which is composed of a bipolar membrane, an acidic anode and an alkaline cathode, with the cation exchange layer (CEL) facing the acidic anode while the anion exchange layer (AEL) facing the alkaline cathode [1,7]. The research team of Xiang and Djilali [7] recently reported that the bipolar membrane fuel cells (BMFCs) have achieved a maximum power density of 327 mW cm^{-2} at 50 °C with dry feed gases. The BMFC showed good stability during 40 h of continuous operation. Ramani [8] reported that the direct borohydride fuel cells (DBFCs) using bipolar composite membranes as polymer electrolyte membranes and liquid hydrogen peroxide as the oxidant yielded a maximum power density of 110 mW cm^{-2}. Each of these bipolar membrane fuel cells used an acidic-alkaline composite membrane as the polymer electrolyte, including a commercial Nafion membrane and a homemade AEM (or using the anion exchange ionomer coating layer as the AEL). Nevertheless, the above-mentioned BMFCs still need to be improved further. One problem is that the costs of the BMFCs are still high because of the use of the expensive Nafion membrane. Another problem is the lifetime of the BMFCs. This kind of acidic-alkaline composite bipolar membrane may split at the junction of the CEL and AEL after long-term operation, owing to the difference of swelling ratio between the cation exchange resin and anion exchange resin. Accordingly, it is essential to prepare a more cost-efficient and integrated bipolar membrane for bipolar membrane fuel cells.

Radiation grafting method is known as one of the effective methods to prepare ion exchange membrane for polymer electrolyte membrane fuel cells [9–15]. Partially fluorinated poly(ethylene-*co*-tetrafluoroethylene) (ETFE) film exhibits superior radiation resistance [16], and has been used as base films for the preparation of ion exchange membranes by graft copolymerization and subsequent sulfonation or quaternarization [17–20]. These polymer electrolyte membranes showed very good mechanical property, chemical stability, thermal stability and fuel cell performance. However, there are few researches about mono-sheet bipolar membranes except one article reported by Fu et al. [21]. They prepared the mono-sheet bipolar membrane by simultaneous irradiation grafting of vinylbenzyl chloride and acrylic acid onto two sides of a porous polyethylene (PE) base membrane, respectively, and subsequent quaternization. The resulting mono-sheet bipolar membranes were used in the field of electrodialysis and showed a voltage drop of 2.0 V at a current density of 80 mA cm^{-2} in 1 mol L^{-1} NaOH aqueous solution. To our best knowledge, no correlative literature about the mono-sheet bipolar membrane applied to fuel cells can be found.

In this work, a new method for the preparation of the mono-sheet bipolar membrane was developed based on pre-irradiation graft copolymerization. Characterizations of the resulting bipolar membranes were carried out by ATR-FTIR, SEM-EDS and TGA, and the ion exchange capacity (IEC), ionic conductivity and water uptake (WU) of the membrane were measured. Besides, the preliminary H_2/O_2 fuel cell tests based on these mono-sheet bipolar membranes were also presented.

2. Experimental

2.1. Materials

The original ETFE base film with the thickness of 30 μm was commercially provided by Asahi Glass Co., Ltd. 1-vinylimidazole (VI, CP, containing 100 ppm hydroquinone as inhibitor) and iodomethane (MeI, CP) were purchased from Beijing Source Fine Chemical Co., Ltd. Styrene (St, CP, containing 100–500 ppm hydroquinone as inhibitor) and iron (II) sulfate heptahydrate ($FeSO_4 \cdot 7H_2O$, AR) were obtained from Xilong Chemical Co., Ltd. 1-vinylimidazole and styrene were distilled under reduced pressure before use. Chlorosulfonic acid was bought from China National Medicines Co., Ltd. The other chemicals were analytical grade and used as received. Deionized water was used throughout this work.

2.2. Membrane preparation

The process for the preparation of the mono-sheet bipolar membranes is shown in Scheme 1, in which four major steps are listed as follows: (1) Pre-irradiation of the ETFE base films, (2) Grafting reaction of the pre-irradiated ETFE base films, (3) Sulfonation of the styrene grafted side (St-Side) of the grafted membranes, followed by hydrolysis reaction, and (4) Alkylation of the 1-vinylimidazole grafted side (VI-Side) of the sulfonated membranes.

2.2.1. Pre-irradiation of the ETFE base films

The ETFE base film samples were washed with acetone, then dried and weighed. After that, the samples were pre-irradiated with the ^{60}Co γ-ray source (Food Research Center of Wanheyuan, Xiamen, China) to the total dose of 100 kGy [17,22] at a dose rate of 4 kGy h^{-1} and ambient temperature under argon atmosphere. The irradiated membranes were stored at −38 ± 2 °C for further use.

2.2.2. Grafting reaction

The pre-irradiated ETFE base films, membrane A, B and C were grafted with the monomer solutions under the protection of nitrogen in a homemade reactor, as shown in Fig. 1. Membrane A was fixed between the Teflon frame ② and ③. Membrane B was fixed between the stainless steel plate ① and Teflon frame ② for measuring the grafting degree of styrene, while membrane C was fixed between the Teflon frame③ and stainless steel plate ④ for measuring the grafting degree of 1-vinylimidazole. Eight holes in each stainless steel plate and Teflon frame were made and the homemade reactor could be fastened by eight bolts. The St solution (20 vol% or 30 vol% St in toluene) and VI solution (87.5 vol% VI aqueous solution containing a certain amount of $FeSO_4 \cdot 7H_2O$) [23] could be injected into the chambers from the inlet ⑤ and ⑥ and contacted with the membranes respectively. The grafting reaction was carried out at 60 °C for 0.5–2 h. The monomers were grafted onto both side of the membrane A simultaneously, thus the St-g-ETFE-g-VI membrane was obtained. Only one side of the membrane B and C was grafted with St or VI monomer. After the reaction, the membranes were washed with organic solvents (methanol for VI-Side and toluene for St-Side, respectively) to remove the low molecular weight homopolymers. Finally, the obtained grafted membrane A, B and C were vacuum dried at 60 °C for 24 h and weighed.

The degree of grafting (DOG) was calculated as follows:

$$DOG\ (\%) = (W_g - W_o)/W_o \times 100\% \qquad (1)$$

where W_g and W_o are the weights of the membrane after and before the grafting reaction, respectively.

DOG-St-VI was determined from membrane A, which was grafted with St and VI onto both side of the membrane. DOG-St or DOG-VI was determined from membrane B or C, which was grafted with St or VI onto one side of the membrane.

2.2.3. Sulfonation reaction

The grafted membranes were fixed in the homemade reactor with the St-Side facing the chlorosulfonic acid solution. In order to reduce the side reaction during the sulfonation, a relatively lower concentration of chlorosulfonic acid solution (2 vol% chlorosulfonic acid in dichloromethane) was used [9]. The membranes were sulfonated at room temperature for 1 h, hydrolyzed in 0.1 mol L^{-1}

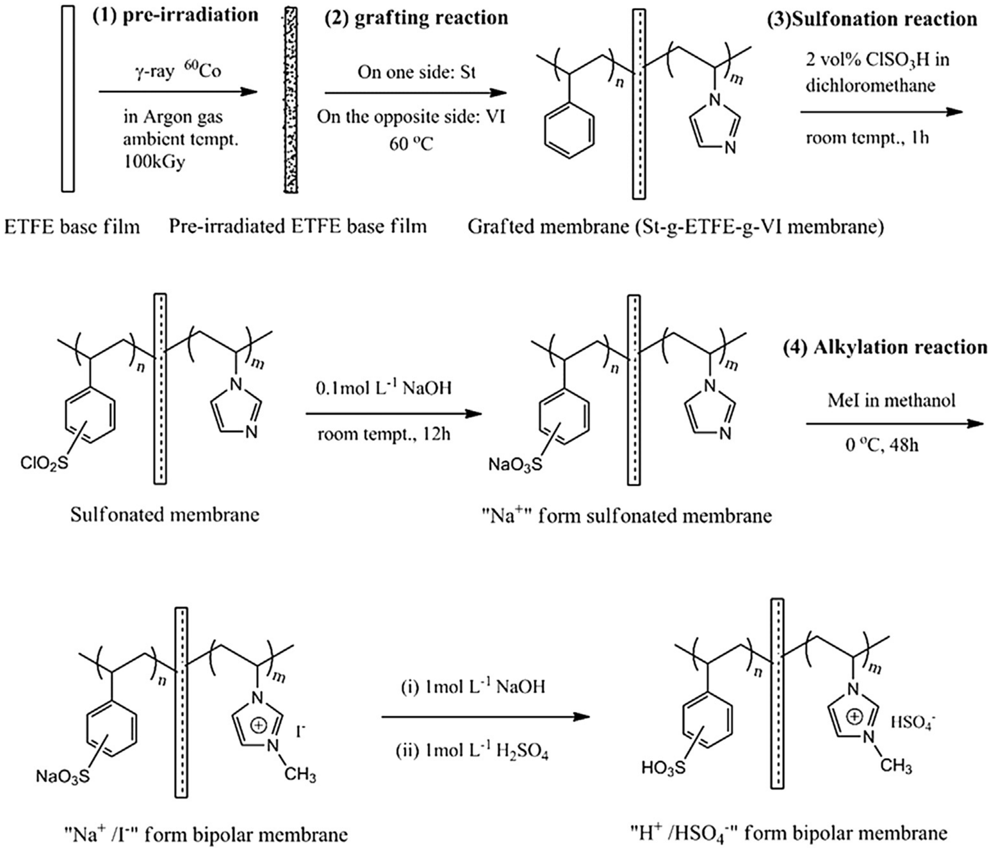

Scheme 1. Preparation process of mono-sheet bipolar membrane based on pre-irradiation grafting method.

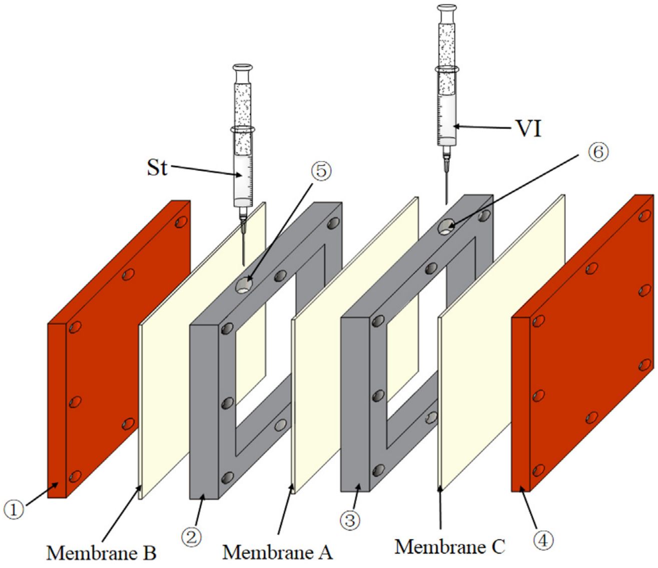

Fig. 1. Schematic diagram of the homemade reactor. ① and ④ are the stainless steel plates, ② and ③ are the Teflon frames with the reagent inlets ⑤ and ⑥, respectively. Membrane A, B and C are the pre-irradiated ETFE base films.

NaOH solution for 12 h, washed with deionized water and finally dried under vacuum at 60 °C for 24 h.

2.2.4. Alkylation reaction

The alkylation reaction was performed by submerging the sulfonated membranes into 50 vol% iodomethane in methanol solution at 0 °C for 48 h. After reaction, the alkylated membranes were rinsed with methanol and deionized water several times, in succession. The resulting "Na^+/I^-" form bipolar membranes were stored in deionized water for further use.

For conversion to the "H^+/HSO_4^-" form, the "Na^+/I^-" form bipolar membranes were immersed in 1 mol L^{-1} NaOH aqueous solution for 24 h, then the "Na^+/OH^-" form bipolar membranes were immersed in 1 mol L^{-1} H_2SO_4 aqueous solution for 48 h with occasional stirring. Finally, the membranes were washed thoroughly with deionized water to remove the residual H_2SO_4.

2.3. Ion exchange capacity

The ion exchange capacity of the bipolar membrane was measured by conventional acid–base titration. For the anion exchange capacity (AEC), the bipolar membranes were alkalized by immersing them into NaOH aqueous solutions (1 mol L^{-1}) at room temperature for 48 h with occasional stirring to transform into "Na^+/OH^-" form, then, the membranes were washed thoroughly to remove the residual NaOH and vacuum dried at low temperature. The dried membranes in "Na^+/OH^-" form were immersed in 25.00 mL of NaCl saturated aqueous solutions for 24 h to exchange OH^- for Cl^-. The solutions containing OH^- originated from the membranes were titrated with 0.01 mol L^{-1} HCl aqueous solution. For the cation exchange capacity (CEC), the "Na^+/Cl^-" form membranes were protonated by immersing them into HCl aqueous solutions (1 mol L^{-1}) at room temperature for 48 h with occasional stirring to transform into "H^+/Cl^-" form, then, the membranes were washed thoroughly to remove residual HCl and vacuum dried at low temperature. The dried membranes in the "H^+/Cl^-" form were immersed in 25.00 mL of NaCl saturated aqueous solutions for 24 h to exchange H^+ for Na^+. The solutions containing H^+ were then titrated with 0.01 mol L^{-1} NaOH aqueous solution. After titration, the resulting "Na^+/Cl^-" form membranes were dried under vacuum at 60 °C for 24 h. IEC (meq g^{-1}) of the membrane can be calculated as follows:

$$\mathrm{IEC}(\mathrm{meq\ g^{-1}}) = (C \times V)/M_{dry} \tag{2}$$

where the C and V are the concentration and volume of HCl or NaOH aqueous solutions for AEC or CEC respectively, M_{dry} is the weight of the dried "Na^+/Cl^-" form bipolar membranes.

2.4. Water uptake

Water uptake was determined by measuring the difference in weight between the dried and wet membranes. Both "Na^+/Cl^-" form and "H^+/HSO_4^-" form bipolar membranes were measured in this work. The membranes were immersed in deionized water for more than 24 h at room temperature. Then the membranes were weighed immediately after the free water on the surface was wiped off. Finally the wet membranes were dried under vacuum at 60 °C until the weights were constant. The water uptake was calculated by the following equation:

$$\mathrm{WU}(\%) = (M_{wet} - M_{dry})/M_{dry} \tag{3}$$

where WU is the water uptake, M_{wet} and M_{dry} are the weight of the wet and dried membranes, respectively.

2.5. Ionic conductivity

The ionic conductivity of the membrane was measured by the two-electrode AC impedance method in ultrapure water (18.25 MΩ cm) using a Parstat 263 electrochemical station (Princeton Advanced Technology, USA) with the AC frequency ranging from 0.1 Hz to 100 kHz. The "Na^+/Cl^-" form bipolar membrane sample was sandwiched between the two stainless steel electrodes and the resistance through the plane was measured, as described in our previous works [24–27]. Before the test, the "Na^+/Cl^-" form membrane samples were soaked in ultrapure water for more than 24 h. The ionic conductivity was calculated as below:

$$\sigma\ (\mathrm{S\ cm^{-1}}) = l/(R \times A) \tag{4}$$

where l (cm) is the length between two potential sensing stainless steel electrodes, R (Ω) is the resistance of the membrane samples, and A (cm^2) is the surface area of the membrane exposed to the electric field.

2.6. Characterizations

The attenuated total reflectance Fourier transform infrared (ATR-FTIR) spectra of the membranes were recorded by a Nicolet iS5 (Thermo Electron Corporation, USA). All the spectra were collected from the dried membrane samples with a resolution of 4 cm^{-1}.

The thermal decomposition behavior of the membranes were investigated by thermo gravimetric analysis (TGA) using a TG209F1 (NETZSCH, Germany) under a nitrogen atmosphere at a heating rate of 10 °C min^{-1} from 30 °C to 600 °C.

The distribution of the sulfur and chlorine elements along the membrane cross-section was analyzed using a Zeiss Sigma scanning electron microscope (SEM) combined with an Oxford X-MAX energy dispersive spectrometer (EDS). All samples were prepared by freeze fracturing the membranes in liquid nitrogen.

2.7. Membrane electrode assembly

The membrane electrode assembly was made up of a bipolar membrane sandwiched between an acidic anode and an alkaline cathode with the CEL facing the acidic anode while the AEL facing the alkaline cathode, and pressed at room temperature under 5 MPa for 5 min. The acidic anode catalyst ink were prepared by mixing isopropyl alcohol, ultrapure water, Nafion solution (5 wt%, EW 1000) and Pt/C catalyst (40 wt%, Johnson Matthey), whereas the homemade soluble anion exchange ionomer [25] was used instead of Nafion solution for the alkaline cathode catalyst ink. The catalyst inks were stirred continuously for 24 h, and sonicated for 15 min, then brushed onto a piece of PTFE-treated carbon paper (Toray-250) and vacuum dried to form the electrode. Pt loading were 0.5 mg cm^{-2} and the weight ratio of Pt catalyst to ionomer was 7:3.

2.8. Fuel cell test

The single cell tests were conducted on a fuel cell test equipment (GEFC-10, Guangdong Electronic Technology Research Institute) with a 4 cm^2 effective area test fixture. For the H_2/O_2 single cell tests, H_2 at the acidic anode and O_2 at the alkaline cathode were fed with the flow rate of 60 mL min^{-1} under 0% relative humidity. Polarization curves were recorded by an integrated electronic load (ZY8714, ZHONGYING Electronic Co., Ltd).

3. Results and discussion

3.1. Preparation of the mono-sheet bipolar membrane

A portion of C—F, C—H and C—C bonds of the ETFE base films were broken after pre-irradiation, leading to the formation of the ETFE radicals. The ETFE radicals can react as active sites with most of the monomers containing double bond. In this work, two different monomers were used to graft onto two sides of the pre-irradiated ETFE membranes, respectively. Styrene was selected as a grafting monomer to prepare the CEL of the bipolar membrane because the phenyl groups can be easily sulfonated with sulfonating agent such as chlorosulfonic acid to introduce sulfonic acid groups, while 1-vinylimidazole was used as another grafting monomer to prepare the AEL of the bipolar membrane owing to the excellent thermal and chemical stability of imidazolium cations under alkaline conditions at high temperature [28,29].

In our preliminary experiments, we found that the graft permeability of St is better than that of VI, as a consequence, the CEL is much thicker than the AEL in the resulting bipolar membrane. So the St solutions at relatively low concentration, 20 vol% and 30 vol% St in toluene, were used at the step of grafting reaction to prepare CEL, while the 87.5 vol% VI aqueous solution containing a certain amount of $FeSO_4 \cdot 7H_2O$ was used to prepare AEL. In order to introduce sulfonic acid groups, the St-Side of the grafted membrane was sulfonated by chlorosulfonic acid as it is highly reactive in electrophilic substitutions of aromatic rings. The sulfonation process was performed at room temperature for 1 h using dichloromethane as the solvent, followed by hydrolysis in 0.1 mol L^{-1} NaOH aqueous solution and deionized water wash.

After the sulfonation process, the 1-vinylimidazole grafted layer of the membrane was alkylated by iodomethane to avoid the formation of extra β-H in the imidazolium salt groups, thus will help to prevent from the Hofmann elimination degradation [30]. The final resulting membrane at its water-saturated state appeared to be tough, orange, translucent and flexible.

3.2. DOG, IEC and WU

The bipolar membrane samples resulting from 20 vol% and 30 vol% St solutions were named as BM1 and BM2 series. Table 1 lists the grafting reaction parameters and the properties of the prepared membranes. As shown in Table 1, each membrane in BM2 series has a higher DOG-St-VI and DOG-St than that in BM1 series for the same grafting reaction time, this is mainly attributed to the higher concentration of St solution, leading to the higher grafting reaction rate. The DOG-St-VI, DOG-St and DOG-VI of all membrane samples increase with the increase of grafting time. The sum of the DOG-St and DOG-VI is approximately equal to the DOG-St-VI when the grafting time is less than 1 h, such as membrane BM1-a, BM2-a, and BM2-b. However, they become gradually unequal as the grafting time is prolonged. This can be explained by the grafting front mechanism [31,32]. According to the front mechanism, grafting reaction initially starts only at the surfaces of the pre-irradiated ETFE base film which contact with the monomer closely. Then the grafted regions swell in the grafting monomer solution, meanwhile the monomer diffuses further into the interior and reacts with the reactive sites of the pre-irradiated ETFE base film. The two grafting fronts covered by different grafting monomer solutions at the two sides of the pre-irradiated ETFE base film continue to move further into the interior of the film as the grafting time increases, ultimately they meet at a certain degree of grafting, which is defined as the graft penetration limit [9]. Based on the above mechanism and our experimental results, the DOG-VI and DOG-St cannot represent exactly the grafting degree of 1-vinylimidazole and styrene of the bipolar membrane respectively when the grafting time is more than 1 h.

The DOG of the membrane is greatly related to the IEC and WU for the radiation-grafted ion exchange membranes. It can be observed from Table 1 that the increase in the DOG-St-VI leads to the increase in the total IEC (the sum of the ACE and CEC) for all membrane samples. This tendency is ascribed to the increase of the number of aromatic rings and imidazole rings at the higher DOG-St-VI, resulting in the increase of sulfonic acid groups and imidazolium cation groups after functionalization. On the other hand, for all membrane samples, the anion exchange capacity is much lower than cation exchange capacity, although the DOG-VI of the membranes is higher than the DOG-St except membrane BM2-b. This is because the ratio of the sulfonation (almost 100% [33,34]) is higher than that of the alkylation. Besides, a small amount of chlorosulfonic acid may penetrate to the VI-Side from the St-Side during the sulfonation and degrade some imidazole groups, resulting in lower anion exchange capacity. The theoretical CEC and AEC can be calculated based on the DOG-St and DOG-VI, and the results are shown in Table S1. Membrane BM1-c and BM2-c exhibit the highest total IEC values of 1.06 and 1.46 meq g^{-1} among the BM1 and BM2 series respectively, showing the appropriate IEC for fuel cell applications.

The water uptake of ion exchange membranes is known to have a profound effect on ion mobility and dimensional stability. Water promotes the ionic transport by solubilizing ions (forming hydrated ions) and broadening aqueous channels in the membrane. However, the high level of water uptake usually reduces the dimensional stability of the membrane. The water uptake results of the six bipolar membrane samples are also shown in Table 1. As expected, the water uptake increases with the increasing DOG-St-VI. This is due to the enhancement of the hydrophilicity of the membranes after inducing the sulfonic acid groups and imidazolium cation groups, and the more ion exchange groups, the stronger hydrophilicity of the membranes. It is seen that even at the DOG-St-VI of 58.84%, the water uptake of the membrane is very low.

3.3. FT-IR spectra

The ATR-FTIR spectra of the original ETFE base film, the St-Side and VI-Side of the St-g-ETFE-g-VI membrane, as well as the CEL and AEL of the bipolar membrane are shown in Fig. 2. The spectrum of

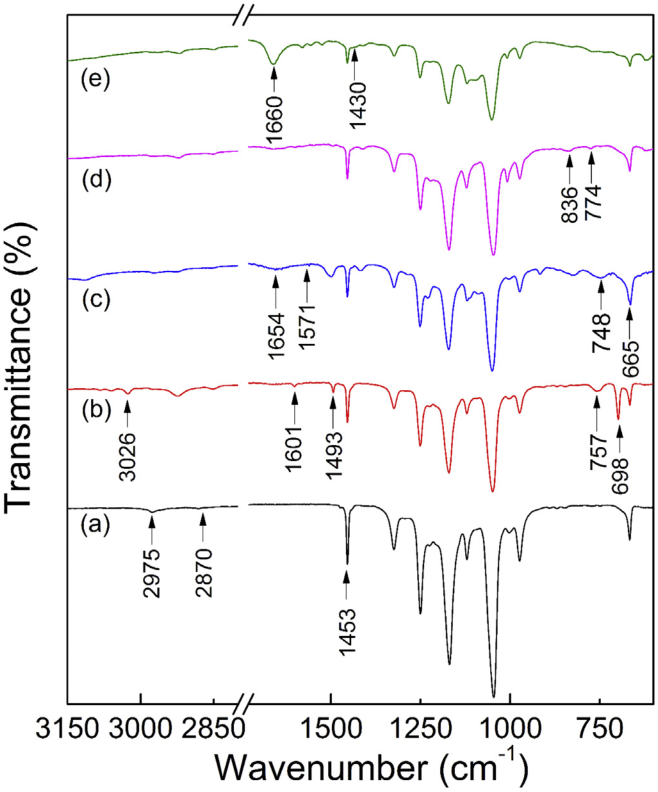

Fig. 2. ATR-FTIR spectra of: (a) the original ETFE base film, (b) the St-Side of the St-g-ETFE-g-VI membrane, (c) the VI-Side of the St-g-ETFE-g-VI membrane, (d) the CEL of the bipolar membrane, and (e) the AEL of the bipolar membrane.

Table 1
Grafting reaction parameters and the properties of the prepared membranes.

Membrane sample	Grafting time (h)	Concentration of St (vol%)	DOG-St-VI (%)	DOG-St (%)	DOG-VI (%)	CEC (meq g^{-1})	AEC (meq g^{-1})	Total IEC (meq g^{-1})	WU (%)	
									"Na^+/Cl^-" form	"H^+/HSO_4^-" form
BM1-a	1	20	23.61	7.73	17.07	0.45	0.34	0.79	5.3	7.3
BM1-b	1.5	20	33.10	12.89	27.83	0.58	0.31	0.89	13.2	14.7
BM1-c	2	20	40.73	17.88	38.55	0.68	0.38	1.06	17.4	17.6
BM2-a	0.5	30	18.07	8.12	9.88	0.59	0.20	0.79	6.0	7.6
BM2-b	1	30	37.13	17.37	17.21	0.90	0.25	1.15	16.7	18.3
BM2-c	2	30	58.84	36.42	37.28	1.23	0.23	1.46	22.9	24.8

the pristine ETFE film displays a strong and broad characteristic band in the range of 1000–1300 cm^{-1} due to the $-CF_2$ stretching vibrations. The aliphatic $-CH_2$ stretching vibration is around 2975 and 2870 cm^{-1} [35], and the sharp band at 1453 cm^{-1} represents the $-CH$ deformation. After grafted, the St-side of the St-g-ETFE-g-VI membrane exhibits a few new absorption bands. The characteristic absorption peak at 1493 and 1601 cm^{-1} are assigned to the vibrations of benzene ring skeleton, 757 cm^{-1} and 698 cm^{-1} are ascribed to the single-substituted benzene ring. As expected, there is no characteristic absorption peak of benzene ring at the VI-Side of the St-g-ETFE-g-VI membrane, and the characteristic peak at 1571, 748 and 665 cm^{-1} identified to the stretching vibration of imidazole ring are found. A small and broad peak at 1654 cm^{-1} may be due to the $-C{=}C$ and $-C{=}N$ stretching vibration. After subsequent functionalization of the St-g-ETFE-g-VI membrane, for the CEL of the bipolar membrane, the single-substituted absorption peaks of benzene ring disappear, moreover, the peaks associated with multi-substituted aromatic units at 836 and 774 cm^{-1} appear, indirectly proving the success of the sulfonation reaction, although it is hard to identify the $O{=}S{=}O$ group whose characteristic peak overlaps with the characteristic peak of $-CF_2$. And in Fig. 2(e), a more sharp and strong adsorption band at around 1660 cm^{-1} is observed compared with Fig. 2(c), which is assigned as the $-C{=}C$ and $-C{=}N^+$ stretching vibration, and the absorption peak at 1430 cm^{-1} is due to the $-CH$ asymmetric deformation vibration of the $-N-CH_3$.

3.4. Thermal stability

Fig. 3 shows the TGA curves of the original ETFE base film, the St-g-ETFE-g-VI membrane and the "Na^+/Cl^-" form bipolar membrane. From Fig. 3(a), it can be seen that the original ETFE base film only has one sharp weight loss commencing at 420 °C, which is due to the decomposition of polymer main chain [36]. For the St-g-ETFE-g-VI membrane, there are two steps of thermal degradation, the first one between 310 and 460 °C is attributed to the degradation of the grafted VI and St groups, and the second one between 460 and 530 °C is the polymer main chain decomposition. As shown in Fig. 3(c), the "Na^+/Cl^-" form bipolar membrane exhibits several steps of thermal degradation: The first slight weight loss (<2.5%) before 200 °C is considered to be the loss of residual water, because the bipolar membrane is more hydrophilic after the sulfonation and alkylation. The second weight loss between 200 and 460 °C is originated from the demethylation, desulfonation, and dearomatization [9]. The third weight loss between 460 and 530 °C is caused by the polymer main chain decomposition. No significant weight loss is recorded below 200 °C, indicating that the bipolar membranes have good thermal stability.

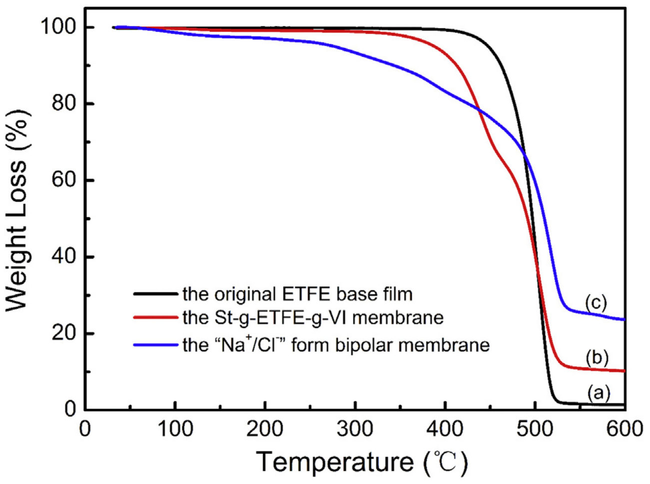

Fig. 3. TGA curves of the membranes.

3.5. Ionic conductivity

Fig. 4(a) shows the ionic conductivity of the "Na^+/Cl^-" form bipolar membranes as a function of temperature. On one hand, the ionic conductivity of the membrane increases with the increasing temperature. This is ascribed to the higher mobility of ions with the higher diffusivity and wider ion transferring channel caused by the flexible and loose membrane structure at higher temperature. On the other hand, an enhancement in the ionic conductivity is observed when the DOG-St-VI of the membrane increases. This growth trend is consistent with the total IEC and the water uptake. So the bipolar membrane BM1-c and BM2-c have the highest ionic conductivity among the BM1 and BM2 series membrane samples, respectively. And for membrane BM2-c, the ionic conductivity goes from 2.12×10^{-2} to 5.32×10^{-2} S cm^{-1} when the temperature varies from 30 °C to 80 °C. It should be pointed out that the ionic conductivity was tested by sandwiching the membrane between the two stainless steel electrodes, therefore the interfacial resistance cannot be ignored because of the large interface between the sample and electrodes, and real ionic conductivity would be higher. In this work, the ionic conductivity of all membranes were measured in "Na^+/Cl^-" form which may be lower than that in "H^+/OH^-" form. To confirm this, the ionic conductivities of the ETFE-g-PSSA proton exchange membranes in Na^+ form and H^+ form (which were prepared by grafting poly(styrene sulfonic acid) onto the ETFE membranes), and the ETFE-g-PMeVI anion exchange membranes in Cl^- form and OH^- form (which were prepared by grafting poly(methyl vinylimidazole) onto the ETFE membranes) were also measured. The results are shown in the Supplementary Material (Fig. S1). It can be seen that the conductivity of ETFE-g-PSSA membrane in Na^+ form is significantly lower than that in H^+ form, and the conductivity of ETFE-g-PMeVI membrane in Cl^- form is slightly lower than that in OH^- form.

The ion transport apparent activation energies of the six fully hydrated membranes were estimated from the linear regression of ln σ vs. 1000/T curve, as shown in Fig. 4(b). Assuming that the ionic conductivity is in compliance with the Arrhenius rules, activation energy (Ea) can be calculated by Eq. (5)

$$Ea = -b \times R \tag{5}$$

where b is the slope of the linear regression of ln σ (S cm^{-1}) vs. 1000/T (K^{-1}) plots and R is the molar gas constant, 8.314 J K^{-1} mol^{-1}. The calculated Ea values of membrane BM1-a, BM1-b, BM1-c, BM2-a, BM2-b and BM2-c are 15.4 ± 0.6, 15.0 ± 0.6, 15.6 ± 0.4, 21.1 ± 0.5, 17.0 ± 0.6 and 15.9 ± 0.2 kJ mol^{-1}, respectively. As we can see, the values are around 16 kJ mol^{-1} except membrane BM2-a (21.1 ± 0.5 kJ mol^{-1}). This is due to membrane BM2-a has the lowest DOG-St-VI among the six membranes, leading to less ionic exchange groups in the interior of the membrane, and finally, resulting in a low ionic conductivity and high apparent activation energy. The apparent activation energies of the ETFE-g-PSSA membrane in Na^+ form and H^+ form, as well as the ETFE-g-PMeVI membrane in Cl^- and OH^- form were also measured for comparison, the results were shown in Fig. S2. It can be seen that the apparent activation energies of H^+ form ETFE-g-PSSA membrane and OH^- form ETFE-g-PMeVI membrane are obviously lower than that of the corresponding Na^+ form and Cl^- form membranes, respectively.

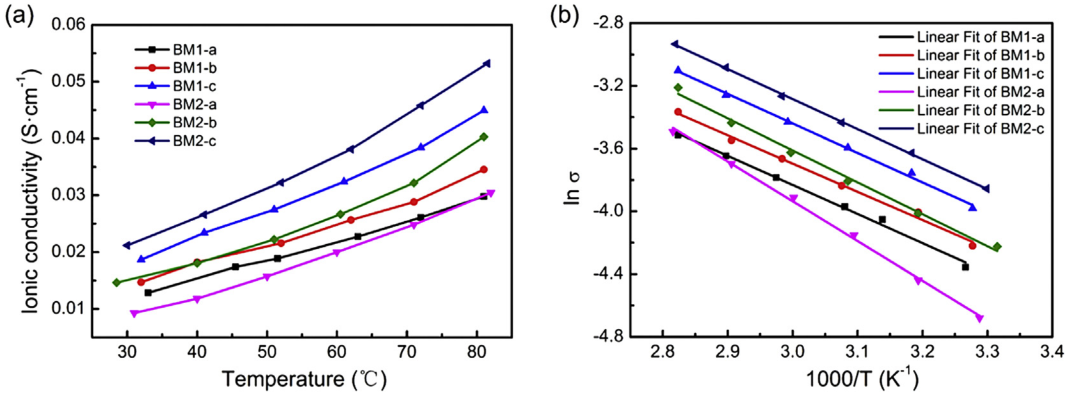

Fig. 4. Temperature dependence of the ionic conductivity.

3.6. SEM-EDS

Fig. 5 shows the cross-sectional distribution of the sulfur and chlorine elements of the "Na$^+$/Cl$^-$" form bipolar membranes. The sulfur element only exists in the sulfonic acid groups while chlorine element emerges in the imidazolium cation groups, therefore, the distribution of CEL and AEL could be reflected by the distribution of the sulfur and chlorine elements. It is found that these membranes have no clear boundary between the CEL and AEL from the SEM-EDS results, indicating the existence of an intermediate layer inside the membrane. An interesting finding is that, for all membrane samples, the thickness of the CEL is much thicker than that of the AEL. And compared with the BM1 series membranes, the CEL of the BM2 series membranes thickens more significantly with the increase of the DOG-St-VI. This is because toluene is a good solvent for polystyrene, which can help St penetrate into deeper layer of the membrane [34]. Another reason may be that the compatibility of styrene with ETFE is better than that of VI.

3.7. Fuel cell test

In order to apply the mono-sheet bipolar membrane to fuel cell, the membrane may be preferably converted into "H$^+$/OH$^-$" form. However, for a "Na$^+$/Cl$^-$" form mono-sheet bipolar membrane, it is hard to replace the cation with proton in the CEL and substitute the anion with hydroxide ion in the AEL simultaneously. Therefore, the "H$^+$/HSO$_4^-$" form bipolar membrane BM1-c and BM2-c were utilized as the polymer electrolyte membrane for the fuel cell test owing to their higher ionic conductivity among the samples. The cell was activated with 100% relative humidity H_2 and O_2 for 9 h, then, tested with dry H_2 and O_2 at 35 °C by closing the humidification system, the iV curve was recorded after the cell operated with dry gases for 15 min. During the fuel cell activation, sulfuric acid may form in the intermediate layer and leach out after some time. Although the cathodic potential is 0.4 V (SHE) under alkaline condition, which is lower than 1.23 V (SHE) under acidic condition, the voltage loss is compensated by the junction potential. Thus the overall cell voltage can also attain to 1.23 V for the bipolar membrane fuel cells in theory [7]. The anodic, cathodic, interfacial and overall reactions are given in Eqs (6)–(9) [6].

$$\text{Anodic reaction: } H_2 \rightarrow 2H^+ + 2e^- \; E^\theta = 0.00\text{V (SHE)} \tag{6}$$

$$\text{Cathodic reaction: } 1/2O_2 + H_2O + 2e^- \rightarrow 2OH^- \; E^\theta = 0.40\text{V (SHE)} \tag{7}$$

$$\text{Interfacial reaction: } 2OH^- + 2H^+ \rightarrow 2H_2O \tag{8}$$

$$\text{Overall reaction: } H_2 + 1/2O_2 \rightarrow H_2O \; E^\theta = 1.23\text{V} \tag{9}$$

Fig. 6 shows the polarization curves and power density curves of

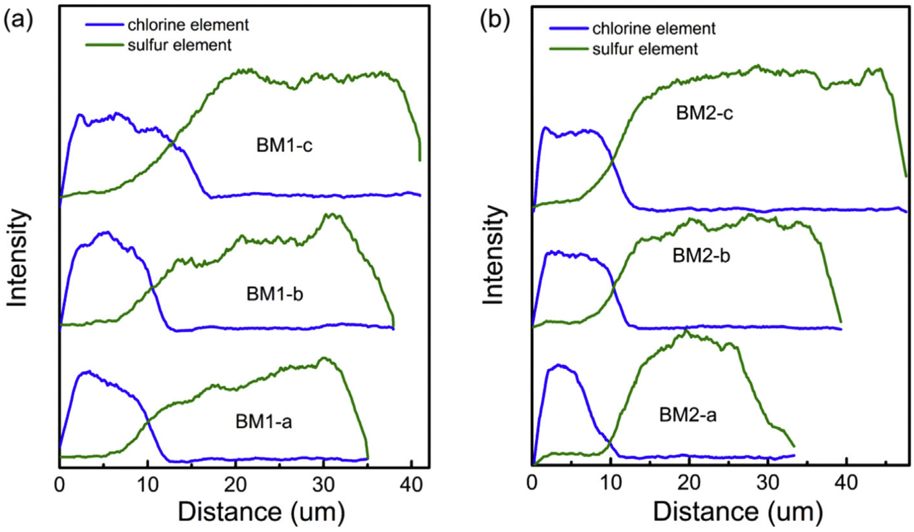

Fig. 5. Element distribution profiles over the cross section of (a) BM1 series bipolar membranes in "Na$^+$/Cl$^-$" form and (b) BM2 series bipolar membranes in "Na$^+$/Cl$^-$" form.

the single cell based on bipolar membrane BM1-c and BM2-c. The open circuit voltage (OCV) of 0.95 V for both single cells was recorded. The high OCV benefited from the low permeability of the reactant gases through the membrane and the compensation of the interfacial potential. The maximum power density of 107 mW cm^{-2} at 260 mA cm^{-2} for BM2-c single cell and 79 mW cm^{-2} at 175 mA cm^{-2} for BM1-c were observed. The single cell with membrane BM2-c had a higher maximum power density was mainly attributed to the higher DOG-St-VI, the total ion exchange capacity and ionic conductivity of membrane BM2-c. We also found that the voltage of the cell decreased gradually with the increasing current density, which was mainly ascribed to the electrode over potentials at high current densities. In this work, we focus on the preparation and characterization of the mono-sheet bipolar membranes, the preparation technique of MEA and operating conditions remain immature and un-optimized, which may limit the performance of the single cell. Future work will be devoted to converting these mono-sheet bipolar membranes into "H^+/OH^-" form as well as the optimization of the MEA fabrication and operating conditions.

4. Conclusions

A new method based on the pre-irradiation grafting technology for the preparation of the mono-sheet bipolar membrane has been developed. A series of bipolar membranes applied to fuel cell have been successfully prepared by simultaneously grafting of St onto one side of the ETFE base film and VI onto the opposite side, followed by the sulfonation and alkylation, respectively. The chemical structures of these membranes were confirmed by ATR-FTIR. The TGA measurements showed reasonable thermal stability of these membranes with a 200 °C onset decomposition temperature. The SEM-EDS results revealed that there was an intermediate layer between the CEL and AEL in the thickness direction, and the CEL was much thicker than the AEL. The ion exchange capacity, water uptake and ionic conductivity of the membranes were also characterized and the values were applicable for fuel cells. The maximum power density of 107 mW cm^{-2} at the current density of 260 mA cm^{-2} and 79 mW cm^{-2} at the current density of 150 mA cm^{-2}, were obtained for H_2/O_2 fuel cells at 35 °C under 0% relative humidity with the bipolar membrane BM1-c and BM2-c, respectively. The above results suggest the great prospect of these membranes for the application of bipolar membrane fuel cells. Future work will be devoted to transforming these membranes into "H^+/OH^-" form and optimization of fabricating the bipolar membrane electrode assembly and operating conditions.

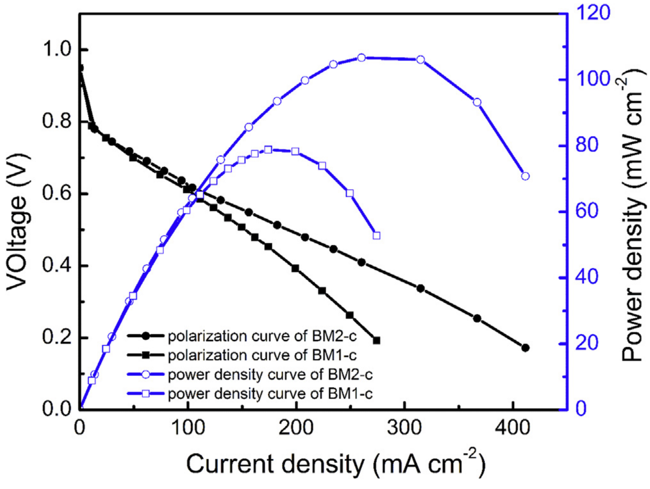

Fig. 6. Performance of the H_2/O_2 single cell with bipolar membrane BM1-c and BM2-c under 0% relative humidity at 35 °C.

Acknowledgement

We gratefully acknowledge the financial support by National Natural Science Foundation of China (Grant Nos., 21376195, 20876129 and 21321062), High-Tech Research and Development Program of China (No. 2008AA05Z107), and National Found for Fostering Talents of Basic Science (No. J1310024).

Appendix A. Supplementary data

Supplementary data related to this article can be found at http://dx.doi.org/10.1016/j.jpowsour.2016.07.060.

References

[1] M. Ünlü, J. Zhou, P.A. Kohl, J. Phys. Chem. C 113 (2009) 11416–11423.
[2] H. Kim, M. Ünlü, J. Zhou, I. Anestis-Richard, P.A. Kohl, J. Power Sources 195 (2010) 7289–7294.
[3] M. Ünlü, J. Zhou, I. Anestis-Richard, P.A. Kohl, ChemSusChem 3 (2010) 1398–1402.
[4] M. Ünlü, J. Zhou, P.A. Kohl, Angew. Chem. Int. Ed. 49 (2010) 1299–1301.
[5] M. Ünlü, J. Zhou, P.A. Kohl, J. Electrochem. Soc. 157 (2010) B1391.
[6] M. Ünlü, J. Zhou, P.A. Kohl, Fuel Cells (2010) 54–63.
[7] S. Peng, X. Xu, S. Lu, P.-C. Sui, N. Djilali, Y. Xiang, J. Power Sources 299 (2015) 273–279.
[8] C.G. Arges, V. Prabhakaran, L. Wang, V. Ramani, Int. J. Hydrogen Energy 39 (2014) 14312–14321.
[9] J. Chen, M. Asano, T. Yamaki, M. Yoshida, J. Membr. Sci. 269 (2006) 194–204.
[10] L. Gubler, M. Slaski, F. Wallasch, A. Wokaun, G.G. Scherer, J. Membr. Sci. 339 (2009) 68–77.
[11] D. Henkensmeier, H. Ben youcef, F. Wallasch, L. Gubler, J. Membr. Sci. 447 (2013) 228–235.
[12] K. Jetsrisuparb, H. Ben youcef, A. Wokaun, L. Gubler, J. Membr. Sci. 450 (2014) 28–37.
[13] S. Kang, D. Jung, J. Shin, S. Lim, S.-K. Kim, Y. Shul, D.-H. Peck, J. Membr. Sci. 447 (2013) 36–42.
[14] S. Kang, D.-H. Jung, J. Shin, S.-K. Kim, Y. Shul, D.-H. Peck, J. Membr. Sci. 459 (2014) 12–21.
[15] T. Zhou, R. Shao, S. Chen, X. He, J. Qiao, J. Zhang, J. Power Sources 293 (2015) 946–975.
[16] J. Chen, M. Asano, Y. Maekawa, M. Yoshida, J. Membr. Sci. 277 (2006) 249–257.
[17] J. Fang, Y. Yang, X. Lu, M. Ye, W. Li, Y. Zhang, Int. J. Hydrogen Energy 37 (2012) 594–602.
[18] L. Gubler, N. Prost, S. Gursel, G. Scherer, Solid State Ionics 176 (2005) 2849–2860.
[19] O.I. Deavin, S. Murphy, A.L. Ong, S.D. Poynton, R. Zeng, H. Herman, J.R. Varcoe, Energy & Environ. Sci. 5 (2012) 8584.
[20] J. Chen, M. Asano, T. Yamaki, M. Yoshida, J. Mater. Sci. 41 (2005) 1289–1292.
[21] R. Fu, T. Xu, W. Yang, Z. Pan, J. Appl. Polym. Sci. 90 (2003) 572–576.
[22] H. Liu, S. Yang, S. Wang, J. Fang, L. Jiang, G. Sun, J. Membr. Sci. 369 (2011) 277–283.
[23] C. Schmidt, G. Schmidt-Naake, Macromol. Mater. Eng. 292 (2007) 1067–1074.
[24] C. Lan, J. Fang, Y. Guan, H. Zhou, J. Zhao, J. Power Sources 295 (2015) 259–267.
[25] M. Guo, J. Fang, H. Xu, W. Li, X. Lu, C. Lan, K. Li, J. Membr. Sci. 362 (2010) 97–104.
[26] H. Xu, J. Fang, M. Guo, X. Lu, X. Wei, S. Tu, J. Membr. Sci. 354 (2010) 206–211.
[27] W. Li, J. Fang, M. Lv, C. Chen, X. Chi, Y. Yang, Y. Zhang, J. Mater. Chem. 21 (2011) 11340.
[28] Y. Ye, Y.A. Elabd, Macromolecules 44 (2011) 8494–8503.
[29] J. Fang, M. Lyu, X. Wang, Y. Wu, J. Zhao, J. Power Sources 284 (2015) 517–523.
[30] J. Fang, P. Shen, J. Membr. Sci. 285 (2006) 317–322.
[31] V.a.c.S. Ivanov, Vsp, Radiat. Chem. Polym. (1992).
[32] H.-P. Brack, H.G. Bührer, L. Bonorand, G.G. Scherer, J. Mater. Chem. 10 (2000) 1795–1803.
[33] J. Chen, M. Asano, T. Yamaki, M. Yoshida, J. Appl. Polym. Sci. 100 (2006) 4565–4574.
[34] Y. Kimura, M. Asano, J. Chen, Y. Maekawa, R. Katakai, M. Yoshida, Radiat. Phys. Chem. 77 (2008) 864–870.
[35] N. Kinger, B.-S. Ko, J.-Y. Sohn, Y.-C. Nho, J. Shin, J. Appl. Polym. Sci. 126 (2012) E349–E357.
[36] A.N. Geraldes, H.A. Zen, G. Ribeiro, H.P. Ferreira, C.P. Souza, D.F. Parra, E.I. Santiago, A.B. Lugão, Radiat. Phys. Chem. 79 (2010) 246–249.